

# Design of a creep resistant iron-base superalloy for Herreshoff furnaces. Part II– Experimental results

Maritza Mariño Cala<sup>1</sup> [mmarino@ismm.edu.cu](mailto:mmarino@ismm.edu.cu)  
Alberto Velázquez del Rosario<sup>1</sup>  
Demetrios Papamantellos<sup>2</sup>  
Apostolos Vasilakus<sup>3</sup>  
Antonio Chang Cardona<sup>1</sup>

## ABSTRACT

Based on the design of a new creep resistant iron-base alloy (Fe-Cr-Ni-C-Al) with the desired properties for the fabrication of Herreshoff furnace arms, samples have been obtained and the influence of heat treatment on microstructure and phase formation has been investigated using both optical and electron microscopy and X-ray diffraction. Mechanical properties at ambient and high temperature have been measured by tensile testing and tensile creep testing. The experimental results are in good agreement with the predictions concerning phase formation, yield stress and creep rupture stress. The target of a lifetime of 100 000 h at 880°C under 180 MPa seems attainable. The design procedure is therefore mainly validated, being promising for design and development of further alloys in our context.

## Key words

Segregation simulation, superalloys, creep, modeling.

<sup>1</sup> Mining-Metallurgy Higher Institute "Dr. Antonio Nunez Jimenez", Moa, Cuba

<sup>2</sup> University of Patras, Greece

<sup>3</sup> Hellenic Centre of Metals Research (ELKEME), Athens, Greece

# **Diseño de una aleación termorresistente base hierro para hornos Herreshoff.**

## **Parte II- Resultados experimentales**

### **RESUMEN**

A partir del diseño de una nueva aleación Fe-Cr-Ni-C-Al con las propiedades deseadas para fabricar brazos de hornos de reducción Herreshoff, se obtuvieron las muestras y se investigó la influencia del tratamiento térmico en la microestructura y la formación de fases utilizando la microscopía óptica y la microscopía electrónica de barrido, conjuntamente con la difracción de rayos X. Se evaluaron las propiedades mecánicas a temperatura ambiente y a altas temperaturas a través de los ensayos de tracción y termofluencia. Los resultados experimentales obtenidos se corresponden con los pronósticos del diseño en lo que respecta a la formación de fases, las tensiones fluencia y las tensiones de rotura demostrando así la posibilidad de obtener una aleación con una durabilidad de 100 000 h a 800 °C bajo tensiones de 180 MPa. Por lo tanto, el procedimiento de diseño empleado es validado y puede considerarse una propuesta novedosa para el diseño y desarrollo de nuevas aleaciones.

### **Palabras clave**

Simulación segregante, superaleación, modelación, termofluencia.

## INTRODUCTION

In part 1 of this series of papers the main mechanical properties of the alloy were predicted using Neural Network models and as quantitative tools to design together with THERMO-CALC Software AB V 2.0 for phase diagram and segregation simulation and the prediction of  $\gamma/\gamma'$  lattice misfit for a new and relatively cheap iron-base superalloy for Herreshoff furnaces applications. However, before manufacturing or using such alloy, it requires to be tested thoroughly to verify whether it actually behaves in the manner predicted. This also serves to validate the use of neural network models in domains where they have not previously been applied.

This alloy is still under experimental investigation, and it will be several years before full mechanical properties tests are completed, in particular long term creep rupture tests. The aim of this work is to conduct microstructural and mechanical testing (including creep tests) have been carried in order to investigate if the alloy matches with predicted properties.

## METHODOLOGY/ANALYSIS

### Alloy production

Ten 20 kg ingots of the designed material were cast produced in a vacuum induction furnace, which reduces the gas and nonmetallic inclusions content. In order to verify the real composition of the alloy, chemical analysis was conducted.

### Samples preparation

The alloy was homogenised for four hours at 1300°C and then water quenched in order to retain the homogeneous austenitic microstructure that facilitates further machining.

Standard tensile creep testing specimens were machined from fully heat treated rods, with a gauge length of 25.4 mm and a diameter of 5.64 mm and later reheated for one hour at 1300°C followed by air cooling to 980°C where it was annealed for five hours. It was then cooled to 850°C and held there for sixteen

hours. These heat treatments are well established to produce fine cuboidal  $\gamma'$  precipitates in the  $\gamma$  matrix with volume fractions between 10 and 15%.

Several alloy samples were filed to powder with approximate particle size of 60mm for the purpose of X-ray analysis. This particle size mitigates the effects of any oxidation at higher temperatures. Prior to X-ray analysis, the powder samples were annealed at 900°C for 20min to remove any mechanical strain produced during filing.

Before and after testing, the metallographic specimens were mechanically polished with SiC paper to a 600 grit finish, and electropolished at 16 V in a 20% perchloric acid-methanol solution at 248 K and then washed successively in methanol and ethanol to be observable using scanning electron microscopy (SEM) or transmission electron microscopy (TEM).

### **Mechanical tests**

The tensile and creep specimens were tested according to ASTM E-139 on an Instron vacuum machine at temperatures of 500 °C, 600 °C, 700 °C and 800°C. Creep tests were performed in constant stress (180 MPa) cam tensile creep machines. Stresses could be applied and maintained to an accuracy of 0.5 %; temperatures were maintained along the gauge length to better than +0.5 K; creep strains were measured with accuracy better than  $10^{-5}$  and displacement curves were recorded with approximately 400 points.

### **X-ray, SEM, EDAX and TEM analysis**

X-ray analysis were carried out to determine the  $\gamma$  and  $\gamma'$  parameters and their corresponding misfit. The X-ray equipment consisted of a Rigaku Rotorflex RU-200 BV diffractometer with a Cu rotating anode and a high temperature vacuum specimen chamber. The anode operated at 55 kV and 180 mA.

Metallographic observations were carried out using conventional optical microscopy, or using SEM or TEM. Energy dispersive X-ray analyses (EDAX) were performed to determine the compositional stoichiometry of different phases. The grain size was estimated by the mean linear intercept technique, as measured from between 300 and 600 grains for each sample.

## RESULTS AND DISCUSSION

### Chemical analysis

The composition of the melt, from chemical analysis, is given in Table 1. It is close to nominal composition except for silicon, which is lower, but this should not affect the mechanical properties much.

Table 1. Chemical composition (wt-%) of the final alloy

Cr	Ni	C	Al	Si	Mn	Fe
23.6	22.1	0.42	1.52	0.83	0.79	50.7

As stated in part I, the best results of simulation corresponded to 1.5 % Aluminium. That's why this amount was taken as nominal composition for the Alloy. The other elements (Cr, Ni, C and Si) were kept in the same quantity.

### Mechanical tests

The tensile and creep test curves are presented in Figures. 1, 2 and 3.

Figures 1 and 2 shows the behaviour of Ultimate Tensile Stress and Yielding Stress after the real tensile test compared with the simulated ones. The values of UTS and YS of the alloy during tests above the temperatures of interest (400°C-800°C) were higher than the predicted. In this case, the tested values are between 4 and 20 percentage above of the expected ones, what probes the accuracy of the neural network model used for simulations.

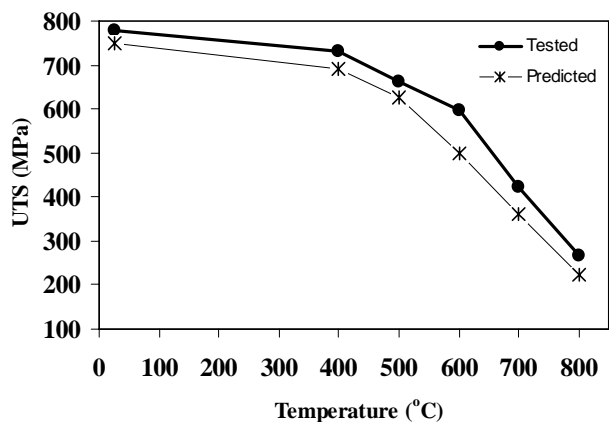


Figure 1. Behavior of the Ultimate Tensile Stress

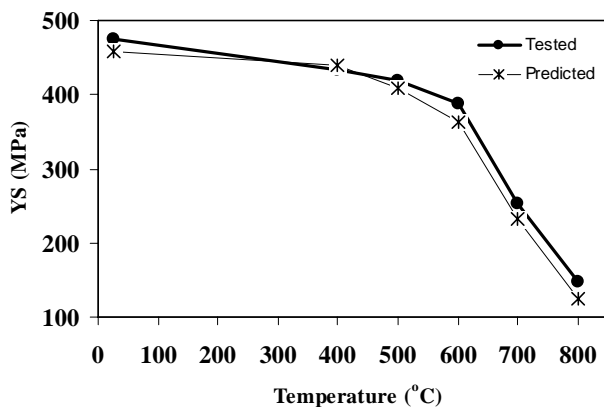


Figure 2. Behavior of the Yield Stress

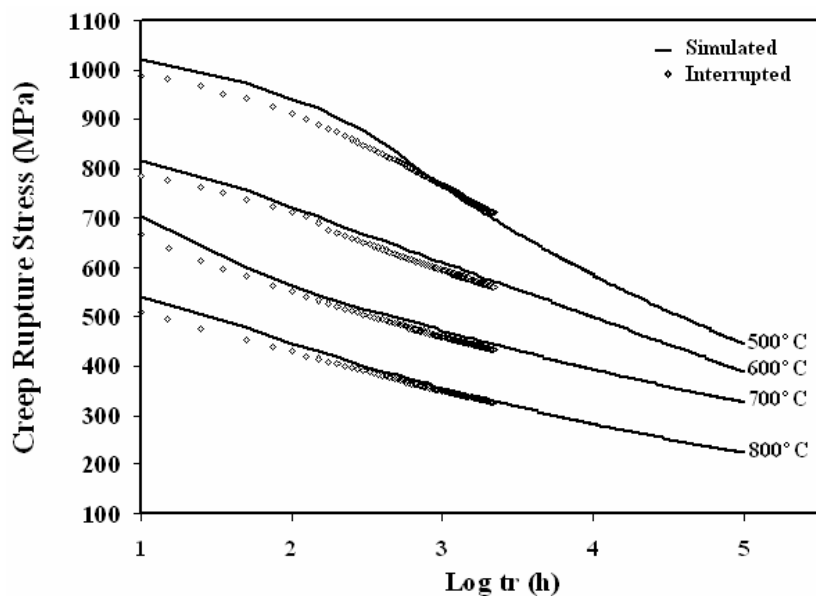


Figure 3. Superimposed curves of tested and simulated crept samples

In Figure 3 can be seen the Creep Rupture Life of the new alloy during creep tests (indicated as stars) compared with the anticipated values (indicated with straight line). It is necessary to highlight that the creep tests were interrupted after 2200 hours. Predicted values are consistent with those expected and found experimentally. As can be seen, the trend for both curves, simulated and tested, is to match themselves when the time is increased.

The predicted relations between creep rupture stress and lifetime satisfies also the design criterion, which demands a creep strength of 180 MPa for 100 000 h at 800°C. In this case, using the Larson Miller parameter for extrapolations and following the trend of the fitted curve for CRL, the alloy is expected to have creep strength around 225 MPa at 800°C, which satisfies the quantitative agreement.

### **X-ray, SEM, EDAX and TEM analysis**

Microstructural analysis reported the presence of  $\gamma$ ,  $\gamma'$  and  $M_{23}C_6$  carbides revealed after EDAX and XRD analysis.  $M_{23}C_6$  carbides corresponds to  $Cr_{23}C_6$  as expected in the design procedure.

Indexed XRD diagram of fully heat treated superalloy (Figure 4) shows peaks corresponding to  $\gamma$ ,  $\gamma'$  and  $M_{23}C_6$  carbides.

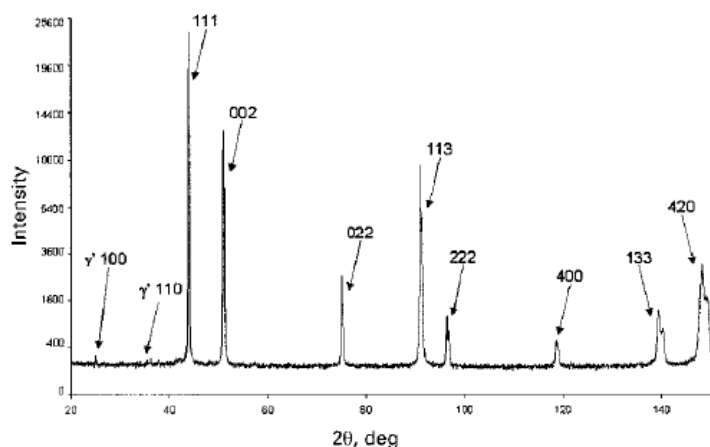


Figure 4. Indexed XRD diagram of fully heat treated superalloy.

Attempts were made to measure lattice mismatch and phase volume fractions using X-ray diffraction (Fig. 4) at the maximum (critical) service temperature (800°C). Owing to an actual small lattice mismatch (with overlapping  $\gamma$  and  $\gamma'$  peaks) and low  $\gamma'$  volume fraction (low  $\gamma'$  peak intensities). Only the (100) and the (110)  $\gamma'$  peaks could be observed as purely superlattice reflections. Figure 5 represents the evolution  $\gamma$  and  $\gamma'$  lattice parameters with temperature.

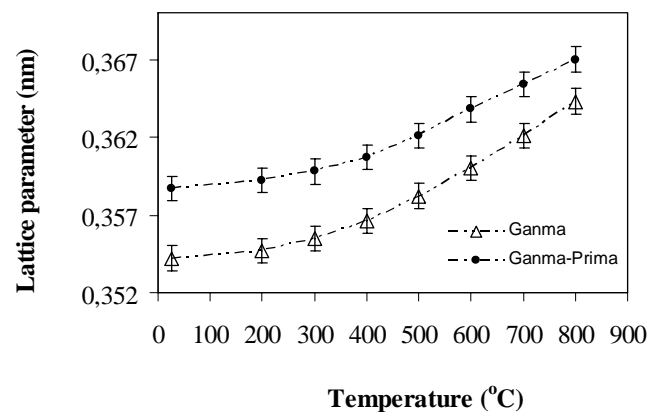


Figure 5. Measured  $\gamma$  and  $\gamma'$  lattice parameters.

The predicted neural network values for lattice misfit varies from + 0.3542 and + 0.3587 at room temperature to + 0.3643 and + 0.367 at 800°C for  $\gamma$  and  $\gamma'$  respectively. As can be seen, the predicted (part I) and measured values are consistent due error bars. The corresponding misfit defined as

$$\delta = 2 \frac{a_{\gamma'} - a_{\gamma}}{(a_{\gamma'} + a_{\gamma})}$$

were calculated from data belonging to Figure 5 and are presented in Figure 6. These low values of misfit improve the creep strength, as expected and revealed mechanical tests.

Phase volume fractions were also estimated roughly by direct comparison (based on peak intensity measurements) and by a Rietveld fitting analysis. Both techniques give a  $\gamma'$  volume

fraction of less than 0.25. TEM and SEM observations show that the  $\gamma'$  volume fraction is also right.

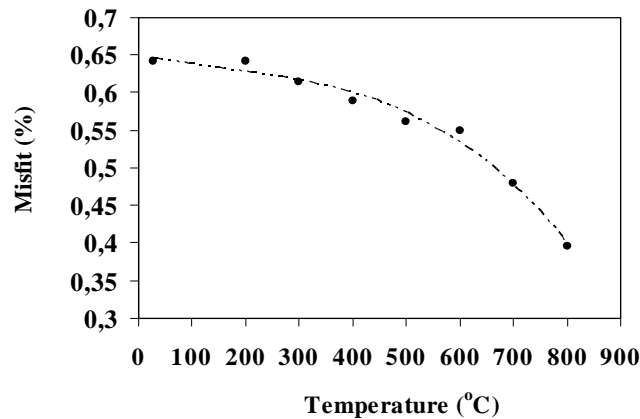


Figure 6. Evolution of  $\gamma / \gamma'$  misfit with temperature.

A typical SEM micrograph of the fully heat treated alloy is presented in Figure. 7.  $\gamma$  (austenitic) matrix with spread rhombohedral  $\gamma'$  particles (light) and a series of lines corresponding to stacking faults with grain boundaries populated with  $\text{Cr}_{23}\text{C}_6$  carbides (dark) which is desirable for good creep resistance due to the  $(\gamma + \gamma' + \text{M}_{23}\text{C}_6)$  decomposition during crystallization and further ageing can be observed.

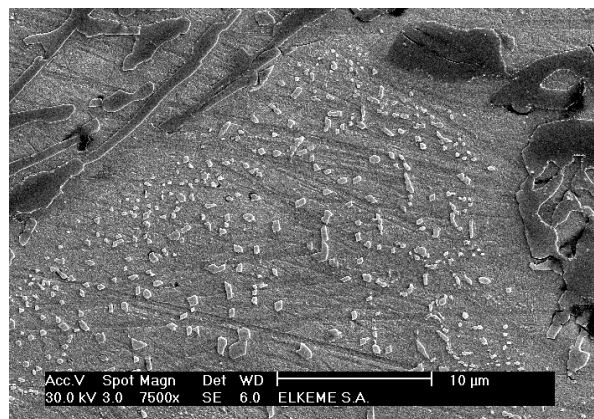


Figure 7. Scanning electron micrographs of fully heat treated samples

$\gamma'$  particles remains stable at high temperature without rafting (Figure 8) ageing twins are also seen, as in many superalloys.

Cubic and tetrahedral  $\gamma'$  precipitates of about 12 nm confirms the existence of low  $\gamma / \gamma'$  lattice mismatch.

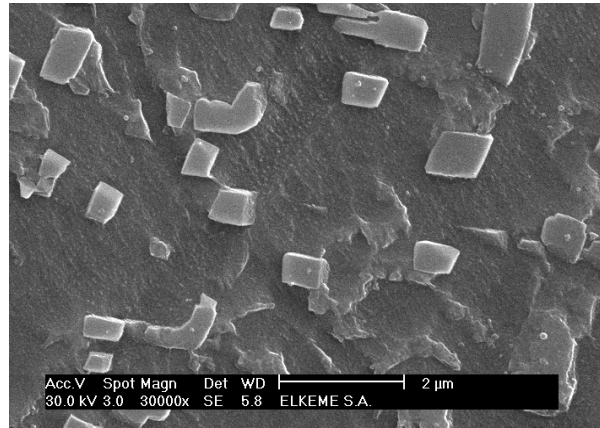


Figure 8. Transmission electron micrographs after tensile test at 800°C.

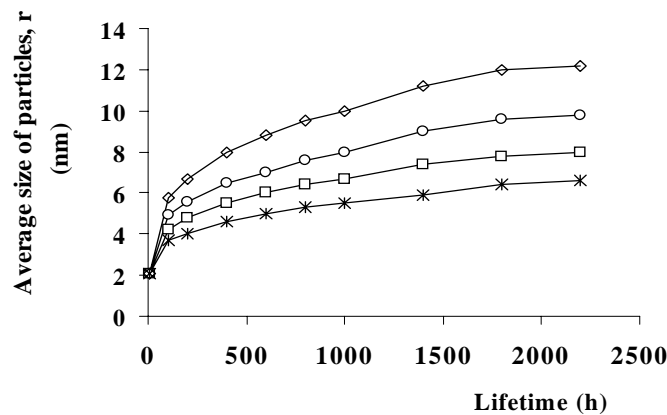


Figure 9. Evolution of  $\gamma'$  average size with time

The average size of particles (Figure 9) increased exponentially when the time was increased, but the maximum size seems to be around 12 nm, which means that there will be not additional risk of decreasing the creep rupture life due to the rafting of increasing of the size of particles. The average grain size of  $\gamma$  resulted to be ASTM 6.35, which matches with the design criteria.

Such experimental results are similar to those obtained by another authors (Tancret et al, 2003; Bhadeshia, 1999; Guo and Sha, 2004; Mandal et al, 2006, Tancret and Bhadeshia, 2003 and Sourmail et al, 2002).

## CONCLUSIONS

A semi-industrial scale cast bar of a newly designed Fe base superalloy has been fabricated and submitted to microstructural, structural, and mechanical investigations, using optical microscopy, SEM, TEM, XRD, tensile testing, and tensile creep testing.

Microstructural and structural characterisations confirmed that the structure of the fully heat treated alloy is close to that expected from both thermodynamical simulation and simple metallurgical considerations: approximately 20 vol. %  $\gamma'$  embedded in  $\gamma$  grains with a small lattice mismatch, and particle like  $\text{Cr}_{23}\text{C}_6$  carbides mainly present at grain boundaries.

All the resulting properties (UTS, YS, Creep strength,  $\gamma$  and lattice parameters,  $\gamma / \gamma'$  mismatch, volume fraction and size of  $\gamma'$  particles and the grain size), are in good agreement with the values predicted by the neural network models developed in Part 1. Although this alloy is still being validated at industrial scale, it is believed that the designed alloy will match the engineering criterion of a creep rupture time of 100 000 h under 180 MPa at 800°C.

The validity and accuracy of the neural network models used as quantitative tools to design a new, suitable and relatively cheap iron-base superalloy for Herreshoff furnaces applications have been demonstrated. The validated design procedure is promising for design and development of further alloys in our context.

## ACKNOWLEDGEMENTS

The authors are grateful to the AAXAL Alfa Network from University of Aachen, Germany, and the Hellenic Centre of Metals Research (ELKEME), Athens, Greece, for funding the project. Our gratitude also goes to Dr. Antonios Katsamas, from Laboratory of Materials, University of Thessaly, Greece for provision facilities for THERMOCALC simulations.

## NOMENCLATURE

$\gamma$  = Austenite

$\gamma'$  = Chemical compound of nickel and aluminium with stoichiometry:  $Ni_xAl_y$

YS = Yield Stress (MPa)

UTS = Ultimate Tensile Stress (MPa)

CRS = Creep Rupture Stress (MPa)

TEM = Transmission Electronic Microscopy

SEM = Scanning Electronic Microscopy

EDAX = Energy Dispersive X-ray analysis

XRD = X-Ray Diffraction

## REFERENCES

- Bhadeshia, H. K. D. H. 1999. Neural networks in materials science. *ISIJ International*, 39 (10) :966-979.
- Guo, Z. y W. Sha. 2004. Modelling the correlation between processing parameters and properties of maraging steels using artificial neural network. *Computational Materials Science*, 29 (1) :12-28.
- Mandal, S., P. V. Sivaprasad, S. Venugopal y K. P. N. Murthy. 2006. Constitutive flow behavior of austenitic stainless steels under hot deformation: artificial neural network modelling to understand, evaluate and predict. *Modelling and Simulation in Materials Science and Engineering*, 14 :1053–1070.
- Sourmail T., H. K. D. H. Bhadeshia y D. J. C. MacKay. 2002. Neural network model of creep strength of austenitic stainless steels. *Materials Science and Technology*, 18 (June) :655-663.
- Tancret, F y H.K.D.H. Bhadeshia. 2003. Design of a creep resistant nickel base superalloy for power plant applications. Part 2–Phase diagram and segregation simulation. *Materials Science and Technology*, 19 (March) : 291-295. .
- Tancret, F, H. K. D. H. Bhadeshia, D. J. C. MacKay, T. Sourmail, M. Yescas, R. W. Evans, C. McAleese, L. Singh and T. Smeeton.2003. Design of creep-resistant nickel-base superalloy for power plant applications. *Materials Science and Technology*, 19 :291-302. Parts 1-3.